Biochemical and Biophysical Research Communications 408 (2011) 52–57

Contents lists available at ScienceDirect

Biochemical and Biophysical Research Communications

journal homepage: www.elsevier.com/locate/ybbrc

Denitrosylation of *S*-nitrosylated OGT is triggered in LPS-stimulated innate immune response

In-Hyun Ryu, Su-Il Do *

Department of Life Science, Laboratory of Functional Glycomics, Ajou University, San 5, Wonchon-dong, Suwon 443-749, Republic of Korea
Department of Molecular Science and Technology, Laboratory of Functional Glycomics, Ajou University, San 5, Wonchon-dong, Suwon 443-749, Republic of Korea

ARTICLE INFO

Article history:
Received 9 March 2011
Available online 29 March 2011

Keywords:
O-linked *N*-acetylglucosaminyltransferase
SNO-OGT
deNO-OGT
Protein *S*-nitrosylation

ABSTRACT

O-linked *N*-acetylglucosaminyltransferase (OGT)-mediated protein *O*-GlcNAcylation has been revealing various aspects of functional significance in biological processes, such as cellular signaling and activation of immune system. We found that OGT is maintained as *S*-nitrosylated form in resting cells, and its denitrosylation is triggered in innate immune response of lipopolysaccharide (LPS)-treated macrophage cells. *S*-nitrosylation of OGT strongly inhibits its catalytic activity up to more than 80% of native OGT, and denitrosylation of OGT leads to protein hyper-*O*-GlcNAcylation. Furthermore, blockage of increased protein *O*-GlcNAcylation results in significant loss of nitric oxide and cytokine production. We propose that denitrosylation of *S*-nitrosylated OGT is a direct mechanism for upregulation of OGT activity by which immune defense is critically controlled in LPS-stimulated innate immune response.

1. Introduction

Since *O*-GlcNAc was discovered [1], it has been known that Ser/Thr-*O*-linked glycosylation (*O*-GlcNAcylation) on a variety of cytosolic and nuclear proteins is catalyzed by *O*-linked *N*-acetylglucosaminyltransferase (OGT) with addition of monosaccharide residue of *N*-acetylglucosamine (GlcNAc) [2,3]. Molecular basis of substrate recognition of OGT and catalysis by OGT has been revealed [4,5], and OGT-catalyzed protein *O*-GlcNAcylation is widely involved in distinct regulation of cellular signaling [6], hyperthermal stress [7], diseases [8,9], and immune systems [10–12]. OGT gene has been cloned in a broad range of species [13–17] and posttranslational modification (PTM) of OGT polypeptide has been reported as two types, such as *O*-GlcNAc modification and tyrosine phosphorylation [13]. Little has been known about influential potency of PTM on OGT catalytic activity and so far, no other type of PTM in OGT protein backbone has been identified.

Innate immune signaling is initiated by specific interaction of pathogen ligands with Toll-like receptors (TLRs) and proinflammatory signaling for antipathogenic defense is triggered to induce nitric oxide (NO) and cytokine production [18,19]. It has been reported that NO, a principle bactericidal mediator is produced primarily by inducible NO synthase (iNOS) under lipopolysaccharide (LPS) stimulation in macrophage cells [20,21]. Moreover, it has been suggested that protein *S*-nitrosylation of cysteine thiols in NO-generating cells could be an important regulator in intracellular signaling [22,23].

In this report, to gain insight into defensive roles of *O*-GlcNAcylation in innate immune stress, we explored the protein *S*-nitrosylation that can control OGT activity in lipopolysaccharide (LPS)-stimulated macrophage cells. Here, we provide the first evidence that OGT was *S*-nitrosylated in resting state and denitrosylation of *S*-nitrosylated OGT (SNO-OGT) is triggered upon LPS stimulation both in vitro and in vivo. Our results show that *S*-nitrosylation together with denitrosylation is previously unrecognized PTM that directly regulates OGT activity in innate immune system.

2. Materials and methods

2.1. Materials

Antibodies for NF_kB p65 (F-6), iNOS (N-20), NOS3 (C-20), actin, PCNA, MBP-tag (N-17), His_6-tag (G-18), and Protein A/G-agarose (PLUS) were purchased from Santa Cruz Biotechnology (Santa Cruz, CA). Antibodies for *O*-linked GlcNAc (RL2) and Streptavidin-HRP were obtained from Abcam (USA) and Vector (USA), respectively. Greiss reagents, Nitrate/Nitrite Assay kit Colorimetric, DON (6-diazo-5-oxo-L-norleucine), OGT antibody (DM17), LPS (*Echerichia coli* 0111), GSNO (*S*-nitroso-glutathione), *p*-nitrophenyl-β-N-Acetyl-glucosamine, PTIO (2-phenyl-4,4,5,5-tetramethylimidazoline-

Abbreviations: OGT, *O*-linked *N*-acetylglucosaminyltransferase; SNO-OGT, *S*-nitrosylated OGT; deNO-OGT, denitrosylated OGT; LPS, lipopolysaccharide; PTM, posttranslational modification; NO, nitric oxide.

* Corresponding author at: Department of Life Science, Laboratory of Functional Glycomics, Ajou University, San 5, Wonchon-dong, Youngtong-gu, Suwon 443-749, Republic of Korea. Fax: +82 31 219 1615.
E-mail address: sido@ajou.ac.kr (S.-I. Do).

0006-291X/$ - see front matter © 2011 Elsevier Inc. All rights reserved.
doi:10.1016/j.bbrc.2011.03.115

1-oxyl 3-oxide), L-MMA(N-methyl-L-arginine), Ascorbate, Neocuproine, and MMTS (*S*-methyl methanethiosulfonate) including all other chemicals for biotin-switch assay were purchased from Sigma–Aldrich Chemical Co. (St Louis, MO). Biotin-HPDP (EZ-Link) and NeutrAvidin-agarose resins were obtained from Thermo (USA). Il-1 beta ELIZA kit was obtained from Invitrogen (USA).

2.2. DNA constructions

Construction of full-length OGT in Flag™-tag mammalian expression vector for recombinant OGT expression (pCMV-OGT-Tag2B), and vector constructions (pET28a(+)-OGT, pET28a(+)-p62) for bacterially expressed his_6-OGT or -p62 were described previously [7].

2.3. Cell culture and transfection

Murine monocytes/macrophage cell line, RAW 264.7 and human macrophage cells, THP-1 were obtained from ATCC (Rockville, MD). Macrophage cells were maintained in DMEM (GIBCO/BRL) media containing 10% fetal bovine serum (Hyclone, UT) supplemented with 100 U/ml penicillin and 100 U/ml streptomycin antibiotics, and were grown as monolayers at 37 °C in a humidified incubator with 5% CO_2 in air. Full-length cDNA encoding rat OGT constructed in pCMV-OGT-Tag 2B (7) was transfected into RAW 264.7 cells using Lipofectamine (Gibco-BRL) according to manufacturer's instructions. Stable single cells were selected with G418 at 400 μg/ml, and OGT expression was screened by gene-specific RT-PCR, and further verified by immunoblotting using flag-tag M2 antibody (Sigma Chemical Co.).

2.4. OGT activity assay

RAW 264.7 cell lysates with and without LPS treatment (100 ng/ml) were prepared in lysis buffer (20 mM Hepes, 1 mM EDTA, 1% NP-40, 0.1 mM neocuproine). His_6-OGT purified by Ni-agarose [7] was treated with 5 mM GSNO in HEN buffer as described [31]. Using cell lysates or his_6-OGT with and without GSNO treatment, OGT activity was assayed with purified his_6-p62 [7], or purified p65 from RAW 264.7 cells, in the presence of 0.5 mM UDP-GlcNAc for 2 h at 37 °C and glycosylation of his_6-p62 or p65 was assessed by RL2 immunoblotting as described[13]. Band intensities of *O*-GlcNAcylated p62 and p65 were quantified by densitometric image analysis and normalized by his_6-p62 and p65 immunoblotting.

2.5. Biotin-switch assay

S-nitrosylation was analyzed by biotin-switch assay as described [26,27]. RAW 264.7 cells were extracted in HEN buffer (250 mM Hepes, 1 mM EDTA, and 0.1 mM Neocuproine, 1% NP-40) for 20 min on ice. Clear extracts were treated in dark condition with 20 mM MMTS in HEN buffer containing 5% SDS at 50 °C for 30 min. Aceton precipitates were treated with biotin-HPDP (0.8 mM) in the presence of 50 mM ascorbate. Excess biotin-HPDP was removed by dialysis, biotinylated proteins were isolated by NeutrAvidin-beads, and analyzed by immunoblotting.

2.6. Immunoblotting analysis

Cells lysates were prepared by sonication in ice-cold lysis buffer (6.7 mM KH_2PO_4, 150 mM NaCl, 0.1% Triton X-100, pH 7.4) and protein samples were resolved by SDS–PAGE under denaturing conditions. Immunoblotting was carried out with *O*-GlcNAc-specific RL2 antibody (1:10,000 dilution, Santa Cruz Biotechnology), or flag-tag-specific M2 antibody (1:15,000 dilution, Sigma Chemical Co.) as described [7]. Protein signal was developed on X-ray Omat-film by ECL (SuperSignal West-Pico chemilumanescent substrate, Pierce).

2.7. Immunoprecipitation

RAW 264.7 cells were extracted in lysis buffer (50 mM Tris–Cl, 150 mM NaCl, 1% NP-40, 1% sodium deoxycholate, 0.1% SDS, 1% BSA, pH 8.0) at 4 °C for 30 min. After centrifugation, clear extracts were incubated with specific antibody (3 μg/ml) at 4 °C overnight. The immune-complex was pulled-down using protein A/G-beads (Santacruz), subjected to SDS–PAGE, and analyzed by immunoblotting.

2.8. Subcellular fractionation

The cytosolic and nuclear fractions from RAW 264.7 cells with and without LPS treatment (100 ng/ml) were prepared by NE-PER® Nuclear and Cytoplasmic Extraction Reagents according to manufacturer's instructions (Thermo, USA).

2.9. Cell viability assay

RAW 264.7 cells treated with LPS (100 ng/ml) or/and DON (1 mM) for the indicated times were suspended in MTT solution (Sigma Chemical Co.) according to manufacturer's instructions and incubated for several hours at 37° C in the CO_2 incubator. After addition of DMSO solution, MTT-treated cells were further incubated at room temperature for 30 min and the signal for live cells was measured by spectrometric absorption at 595 nm.

2.10. Griess assay

Culture media from RAW 264.7 cells treated with LPS (100 ng/ml) for the indicated times were treated with Griess solution (1% sulfanilamide, 0.1% naphthylethylenediamine dihydrochloride, and 2% phosphoric acid) for 10 min at room temperature and measured the amount of nitrite (NOO^-) by spectrometric absorption at 570 nm as described [28]. Total NO (nitrate and nitrite) was measured by Nitrate/Nitrite Assay kit Colorimetric according to manufacturer's protocols (Sigma Co.). Briefly, culture media from RAW 264.7 cells treated with LPS were pre-reacted with nitrate reductase and its co-factor for 2 h at room temperature followed by same treatment with Griess solution as mentioned above. Amount of nitrate ($NOOO^-$) and nitrite (NOO^-) was determined by spectrometric absorption at 570 nm.

2.11. Measurement of cytokines

Culture media from RAW 264.7 cells treated with LPS (100 ng/ml) for the indicated times were collected and the released cytokines including IL-1β were assayed by cytokine-specific Eliza Kit according to manufacturer's instructions (Biosource).

2.12. Purification of p65

RAW 264.7 cells were extracted in RIPA buffer (50 mM Tris–Cl, 150 mM NaCl, 1% NP-40, 0.5% sodium deoxycholate, 0.1% SDS, 1 mg/ml BSA, pH 7.0) at 4 °C for 30 min. After centrifugation, clear extracts were incubated with p65 antibody (5 μg) overnight in cold room. Immune-complex was isolated with protein AG-beads at 4 °C for 2 h. PBS-washed immune-complex was treated with 0.1 M Glycine buffer (pH 2.5), and the released p65 was dialyzed in ice-cold PBS buffer overnight.

2.13. Isolation of peritoneal macrophages in vivo

Mice (BALB/c) were injected intraperitoneally (i.p.) with 1 ml of 4% F-TG (F-thioglycollate, SIGMA) for 2–3 days, further injected with and without LPS (1 g/kg body wt.) for the indicated times, and macrophages were obtained through washing the peritoneal cavity with cold sterile PBS followed by centrifugation at 170*g* for 5 min as described [25]. The collected peritoneal macrophages were used either for immunoblot analysis or cultured ex vivo.

3. Results and discussion

3.1. Enhanced protein O-GlcNAcylation in LPS-treated macrophage cells in vitro and in vivo

To investigate whether cellular level of protein *O*-GlcNAcylation was changed during in vitro LPS stimulation of RAW264.7 cells, we analyzed *O*-GlcNAcylation by RL2 immunoblotting. Protein *O*-GlcNAcylation was initiated to be increased at early phase of 2 h, maximized at 12 h LPS treatment, and this enhanced *O*-GlcNAcylation

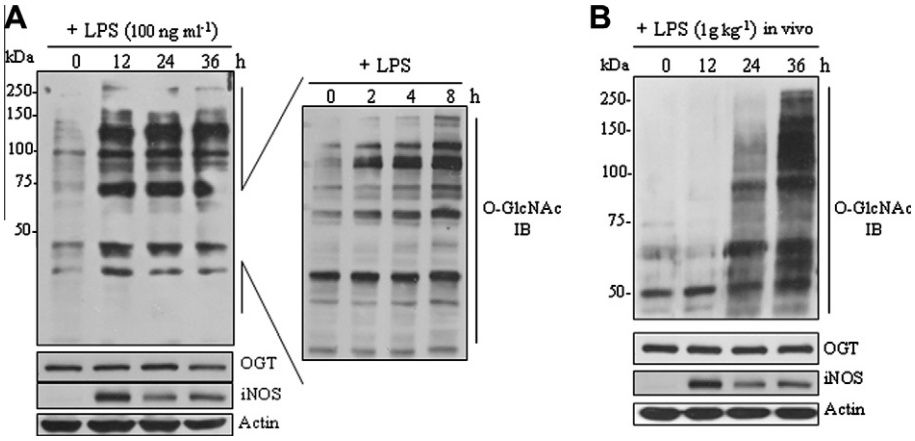

Fig. 1. Time-dependent LPS stimulation elicits enhanced protein *O*-GlcNAcylation in macrophage cells in vitro and in vivo. Immunoblot analysis of protein *O*-GlcNAcylation (indicated *O*-GlcNAc IB) of whole cell lysates from LPS-treated RAW 264.7 cells (100 ng/ml) in vitro (A), and from peritoneal macrophages of LPS-injected mice (1 g/kg body weight) in vivo (B) for the indicated time periods. Endogenous OGT, iNOS, and actin were immunoblotted as indicated.

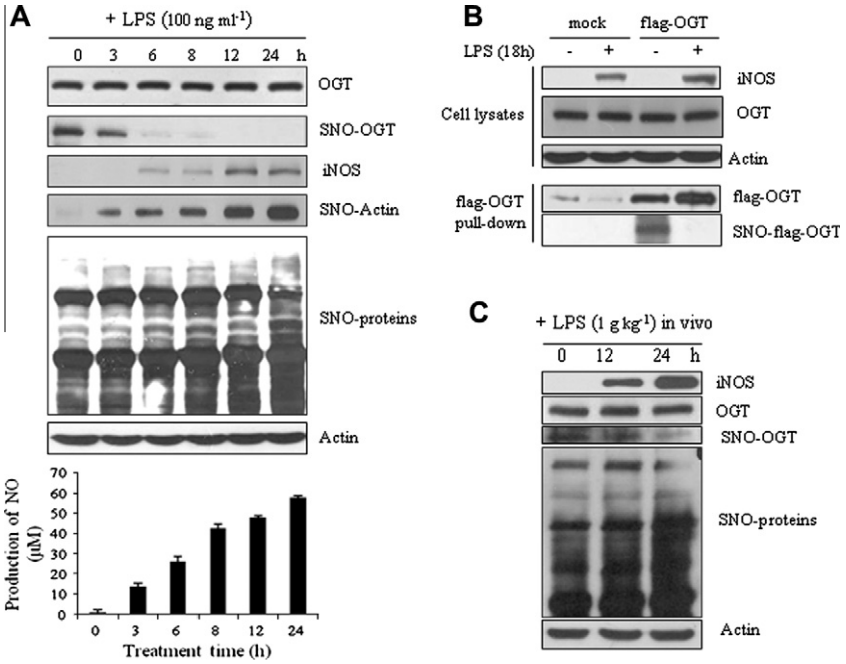

Fig. 2. Denitrosylation of SNO-OGT is triggered by LPS stimuli in macrophage cells in vitro and in vivo. (A) Biotin-switch assay-coupled immunoblot analysis of protein *S*-nitrosylation of OGT (SNO-OGT) together with *S*-nitrosylation of cellular proteins (SNO-proteins) and actin (SNO-actin) in LPS-treated RAW 264.7 cells in vitro for the indicated times. Total NO production during LPS treatment was monitored by Griess assay after nitrate reduction (bottom panel) and data are presented as mean ± s.e.m.; ($n = 3$). (B) Biotin-switch assay-coupled immunoblot analysis of protein *S*-nitrosylation of pull-down flag-OGT (SNO-flag-OGT) by biotin-switch assay in cell lysates from control cells and stably transfected cells expressing recombinant flag-tagged OGT without or with LPS treatment in vitro for 18 h. (C) Biotin-switch assay-coupled immunoblot analysis of protein *S*-nitrosylation of OGT, and cellular proteins in peritoneal macrophages from LPS-injected mice in vivo for the indicated periods. Endogenous OGT, iNOS, and actin were immunoblotted as indicated.

was prolonged until 24 h LPS treatment whereas endogenous OGT level was not affected (Fig. 1A). Expression pattern of inducible NO synthase (iNOS) was consistently observed with previous studies of LPS-activated mouse macrophage cells [24]. We further analyzed the in vivo influence of LPS treatment on protein *O*-GlcNAcylation. Mice were intraperitoneally injected with LPS for the given times, peritoneal macrophages were collected [25], and protein *O*-GlcNAcylation was analyzed by immunoblotting. Strongly enhanced protein *O*-GlcNAcylation with no significant change of OGT level was observed in vivo similarly as in vitro LPS treatment (Fig. 1B). Together, these results suggest that increased protein *O*-GlcNAcylation is elicited by LPS signaling cascades during innate immune response, and some qualitative, rather quantitative aspects of OGT may be responsible for this enhanced protein *O*-GlcNAcylation.

3.2. LPS stimuli-triggered denitrosylation of SNO-OGT in vitro and in vivo

To dates, any PTM of OGT by which enzyme activity is directly controlled has not been identified. To this end, we sought to determine if OGT was covalently modified with NO during LPS treatment of RAW264.7 cells. We analyzed protein *S*-nitrosylation by biotin-switch assay [26,27], and total NO production was monitored by Griess assay after nitrate reduction during LPS treatment [28]. Notably, it was of great interest to find that OGT was *S*-nitrosylated in a resting state before LPS stimulation, and *S*-nitrosylated OGT (SNO-OGT) was gradually denitrosylated depending on LPS treatment with no change of OGT level (Fig. 2A). Evidently, *S*-nitrosylation of actin [26] and cellular proteins was increased in parallel with NO production during LPS treatment (Fig. 2A). To further validate this finding, recombinant flag-OGT was expressed in RAW264.7 cells, and *S*-nitrosylation of flag-OGT was analyzed by biotin-switch assay. Clearly, flag-OGT trapped in pull-down beads was found to be *S*-nitrosylated before LPS treatment, and it was completely denitrosylated after LPS treatment (Fig. 2B). We next performed in vivo analysis of SNO– and deNO-OGT by biotin-switch assay. Macrophages were isolated from intraperitoneally LPS-injected mice, and protein *S*-nitrosylation was analyzed by biotin-switch assay. Indeed, OGT was present as SNO-form in resting state, and denitrosylation was processed upon LPS stimulation in vivo as in vitro (Fig. 2C). Taken together, these findings demonstrate that OGT exists as SNO-form in resting state, and denitrosylation is triggered by LPS stimuli in macrophage cells. SNO-form of OGT reflects a novel type of PTM in case of OGT, which is previously unrecognized. It is of particular that denitrosylation of SNO-OGT is exerted under NO-producing environment that actin is strongly *S*-nitosylated (Fig. 2A). These results indicate two possibilities that first, considering the enhanced *O*-GlcNAcylation in LPS treated cells, catalytic activity of SNO-OGT in resting state can be considerably repressed compared to that of deNO-OGT in LPS stimulation, and secondly, LPS-stimulated removal of NO from

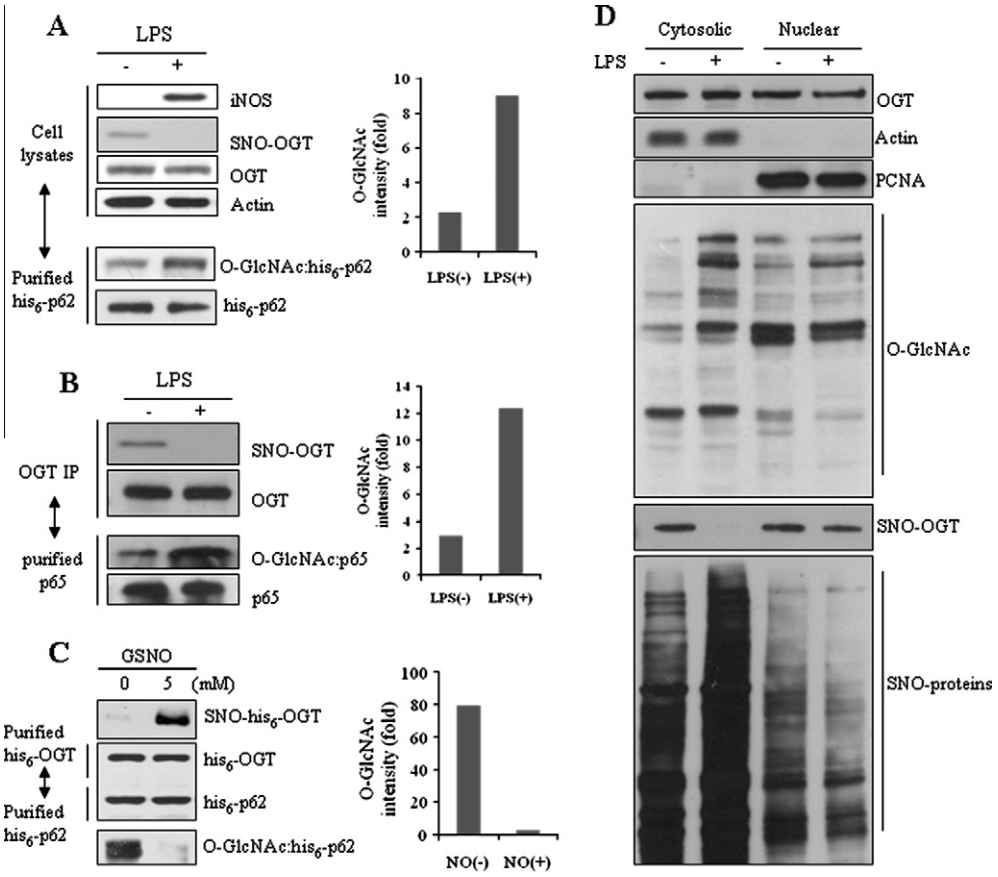

Fig. 3. Upregulation of OGT catalytic activity by denitrosylation of SNO-OGT and cytosol-specific denitrosylation of SNO-OGT. OGT catalytic activity of cell lysates from control and LPS-treated RAW 264.7 cells was assessed by *O*-GlcNAcylation of recombinant p62 ($n = 3$) (A), and by *O*-GlcNAcylation of purified p65, NF_kB subunit ($n = 3$) (B). (C) SNO-OGT was generated by incubation of recombinant OGT with GSNO (*S*-nitroso-glutathione) and its enzyme activity was assessed by *O*-GlcNAcylation of recombinant p62 ($n = 3$). Arrow indicates source of enzymes (upper) and substrates (lower) in OGT reaction. Reaction product of *O*-GlcNAcylated-p62 or -p65 was immunoblotted using anti-*O*-GlcNAc Antibody (RL2) (A-C) and OGT activity was relatively quantified by image analysis of RL2 immunoblottings and normalized by immunoblotted p62 or p65 substrate used in OGT reaction (Each right panel of A, B, and C; Bar indicates average value of triplicates.). (D) Immunoblot analysis of *O*-GlcNAc level, and biotin-switch assay-coupled immunoblot analysis of protein *S*-nitrosylation of OGT (SNO-OGT) and cellular proteins (SNO-proteins) in cytosolic and nuclear fractions from RAW 264.7 cells before and after 100 ng/ml LPS treatment for12 h. Endogenous OGT, PCNA (control for nuclei), and actin (control for cytosols) was immunoblotted as indicated.

SNO-OGT might be facilitated against high NO gradient in a specified microenvironment.

3.3. Upregulation of OGT catalytic activity via cytosol-specific denitrosylation of SNO-OGT

First, to address the former possibility, we examined the OGT activity both in resting and LPS-stimulated RAW264.7 cells. Catalytic activity of SNO-, and deNO-OGT was assessed by the glycosylation of purified his_6-p62 [7] and purified p65 of NF_kB subunit, demonstrating that deNO–OGT showed more than four fold, and six fold higher activity compared to SNO-OGT, respectively (Fig. 3, A and B). To further confirm these results, his_6-OGT was expressed in *E. coli* [7] and *S*-nitrosylated in vitro with *S*-nitroso-glutathione (GSNO) treatment as described [29]. *S*-nitrosylation of his_6-OGT with GSNO was performed in a concentration dependent manner, and NO production was monitored by Griess assay (results not shown). Enzyme activity of native his_6-OGT and SNO-his_6-OGT trapped in pull-down beads was assessed by his_6-p62 glycosylation, demonstrating that SNO-his_6-OGT exhibited about eighty fold less activity compared to native his_6-OGT (Fig. 3C). Taken together, these results clearly indicate that NO attachment to OGT results in strongly reduced catalytic activity whereas NO removal recovers OGT activity. Secondly, to address the latter possibility, we investigated subcellular localization of SNO-OGT, and determined whether denitrosylation of SNO-OGT occurred in cytosol or nucleus. We separated cytosolic and nuclear fractions, and SNO- and deNO-OGT were analyzed by biotin-switch assay. Immunoblots of actin and PCNA were utilized as cytosol- and nucleus-specific controls. As shown in Fig. 3D, in resting state, SNO-form of OGT was almost equally localized in both cytosolic and nuclear fractions whereas about 40% of total OGT was localized in nuclear fractions with remaining 60% in cytosolic fractions. Interestingly, however, cytosolic SNO-OGT, not nuclear SNO-OGT was predominantly denitrosylated even under the condition of increasing cellular SNO-proteins by LPS treatment (Fig 3D). In parallel, protein *O*-GlcNAcylation was significantly increased in cytosol, not in nucleus (Fig 3D). These results support the idea that LPS-stimulated mechanism of OGT denitrosylation must be operated in a distinct molecular complex at cytosolic milieu, and denitrosylation of cytosolic SNO-OGT can directly link to enhanced cytosolic protein *O*-GlcNAcylation.

3.4. Suppression of NO and cytokine production by DON-treated attenuation of protein hyper-O-GlcNAcylation

To explore the biological significance of increased protein *O*-GlcNAcylation, we determined whether the blockage of enhanced protein *O*-GlcNAcylation affected NO and cytokine production. To do this, we treated RAW264.7 cells with DON as described [7] to attenuate the increased protein *O*-GlcNAcylation during LPS treatment. LPS-enhanced cellular protein *O*-GlcNAcylation was markedly abrogated by DON treatment (Fig. 4A) and simultaneously, iNOS expression as well as production of interleukin 1β (IL-1β) and NO were significantly inhibited (Fig. 4, A–C). In addition, DON-treated cells survived about two fold more efficiently than control cells during LPS treatment (Fig. 4D). These findings suggest that protein hyper-*O*-GlcNAcylation during LPS-stimulated innate immune response is critically functioning to cause sufficient induction of iNOS, and efficient production of cytokines and NO although NO has a deleterious effect on cell survival itself. More importantly, we next examined *O*-GlcNAcylation of NF_kB and its ef-

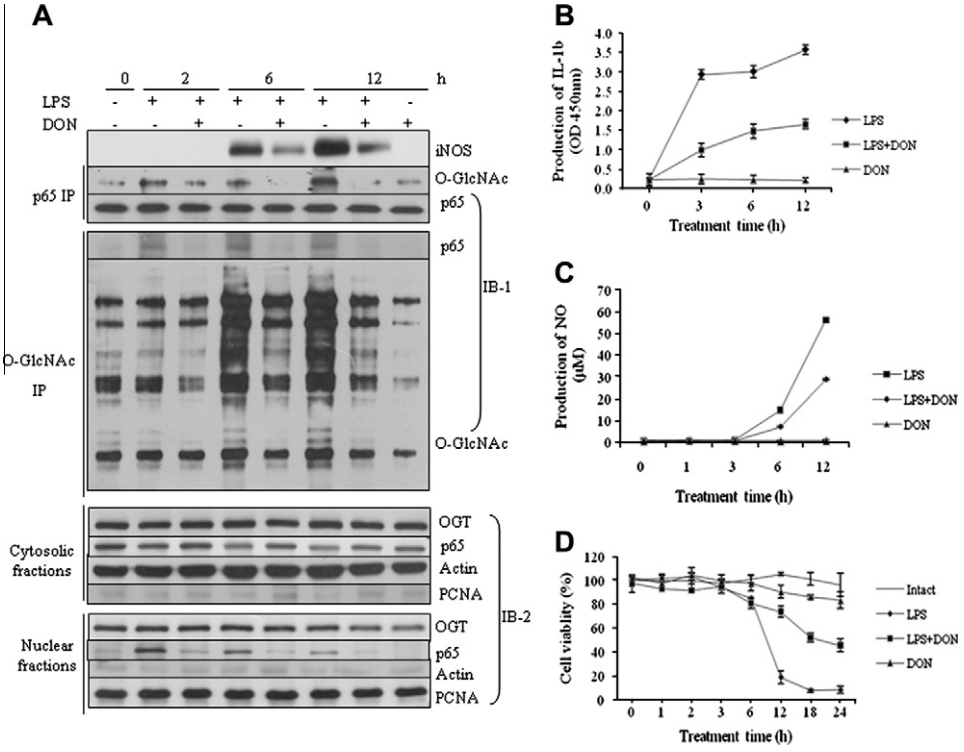

Fig. 4. Inhibition of protein hyper-*O*-GlcNAcylation diminishes nuclear translocation of NF_kB and results in reduced production of IL-1β and NO. (A) Immunoblot analysis of immunoprecipitated-p65 (p65 IP) and -*O*-GlcNAc-containing proteins (O-GlcNAc IP) using p65 antibody and RL2 in whole cell lysates from control, and 100 ng/ml LPS-treated RAW 264.7 cells in the absence or presence of 1 mM DON treatment for the indicated times (IB-1). During the same treatment, cytosolic and nuclear fractions were separated, and subjected to immunoblot analysis of p65 (IB-2). Endogenous OGT, iNOS, PCNA, and actin were immnunoblotted as indicated. Effect of DON treatment on IL-1β production ($n = 5$) (B), total NO production after nitrate reduction ($n = 3$) (C), and cell survival ($n = 3$) (D) during LPS treatment of RAW 264.7 cells. Error bars in (B–D) are presented as mean ± s.e.m.

fect on NF_kB nuclear translocation, since NF_kB was a major transcriptional factor responsible for cytokine and NO production in immune systems [30]. As shown in Fig. 4A, in resting state, NF_kB *O*-GlcNAcylation was weakly detected as a basal level and most NF_kB was found in cytosolic fractions. Upon LPS treatment, NF_kB *O*-GlcNAcylation was significantly increased, and a certain portion of NF_kB was found in nuclear fractions. However, this situation was reversed by DON treatment, demonstrating that abrogation of LPS-enhanced *O*-GlcNAcylation of NF_kB by DON treatment inhibited NF_kB nuclear translocation (Fig. 4A). These results are consistent with previous reports suggesting that NF_kB activation is closely associated with *O*-GlcNAcylation [9,12]. Taken together, these findings suggest that attenuation of protein hyper-*O*-GlcNAcylation diminishes NF_kB nuclear translocation, which results in reduced iNOS expression, and significant loss of IL-1β and NO production.

Our results, for the first time, demonstrate that OGT exists as SNO-form in resting state of RAW264.7 cells, and SNO-OGT becomes deNO-form through a cytosol-specific denitrosylation mechanism that is triggered in LPS stimulated innate immune response (S. Fig. 1). Our findings also provide the first evidence that conversion of SNO- to deNO-OGT is up regulatory mechanism of OGT catalytic activity and deNO-OGT is critically functioning for innate immune defense through eliciting protein hyper-*O*-GlcNAcylation. It has been generally recognized that cellular SNO-proteins are constitutively maintained with a basal level of NOS activity through several specific mechanisms in mammalian system [22,23,31]. However, denitrosylation mechanism of SNO-proteins is not fully understood whether it is chemically redox-based [26,32,33], enzymatic with protein-based [34–36], or facilitated by unidentified mechanism. Molecular elucidation of denitrosylation mechanism of OGT may provide a novel understanding about NO removal pathway in LPS-stimulated innate immune response. Furthermore, dysregulation of denitrosylation mechanism of OGT may link to malfunction of innate immune systems.

Acknowledgments

We thank Dr. Ki-Young Lee (GG Pharmaceutical Institute) for helpful discussion and critical reading of the manuscript; Il-Soo Shin (Ajou University) and Jee-Haeh Do (Seoul National University) for providing technical assistance. This work was supported by Glycomics Research Project Grants (No. 20100002028, GRP 2008-2012) from Korea Science and Engineering Foundation & National Research Foundation of Korea.

Appendix A. Supplementary data

Supplementary data associated with this article can be found, in the online version, at doi:10.1016/j.bbrc.2011.03.115.

References

[1] C.R. Torres, G.W. Hart, Topography and polypeptide distribution of terminal *N*-acetylglucosamine residues on the surfaces of intact lymphocytes. Evidence for *O*-linked GlcNAc, J. Biol. Chem. 259 (1984) 3308–3317.
[2] D.C. Love, J.A. Hanover, The hexosamine signaling pathway: deciphering the '*O* -GlcNAc code', Sci. STKE 312 (2005) 1–14.
[3] G.W. Hart, M.P. Housley, C. Slawson, Cycling of *O*-linked beta- *N*-acetylglucosamine on nucleocytoplasmic proteins, Nature 446 (2007) 1017–1022.
[4] M. Jinek, J. Rehwinkel, D. Lazarus, E. Izaurralde, J.A. Hanover, E. Conti, The superhelical TPR-repeat domain of *O*-linked GlcNAc transferase exhibits structural similarities to importin alpha, Nat. Struct. Mol. Biol. 11 (2004) 1001–1007.
[5] A.C. Clarke, R. Hurtado-Guerrero, S. Pathak, A.W. Schuttelkopf, V. Borodkin, S.M. Shepherd, A.F. Ibrahim, D.M. van Aalten, Structural insights into mechanism and specificity of *O*-GlcNAc transferase, EMBO J. 22 (2008) 2780–2788.
[6] L. Well, K. Vosseller, G.W. Hart, Glycosylation of nucleocytoplasmic proteins: signal transduction and *O*-GlcNAc, Science 291 (2001) 2376–2378.
[7] K.-C. Sohn, K.-Y. Lee, J.-E. Park, S.-I. Do, OGT functions as a catalytic chaperone under heat stress response: a unique defense role of OGT in hyperthermia, Biochem. Biophys. Res. Commun. 22 (2004) 1045–1051.
[8] X. Yang, P.P. Ongusaha, P.D. Miles, J.C. Havstad, F. Zhang, W.V. So, J.E. Kudlow, R.H. Michell, J.M. Olefsky, S.J. Field, R.M. Evans, Phosphoinositide signaling links *O*-GlcNAc transferase to insulin resistance, Nature 451 (2008) 964–969. 2008.
[9] L.R. James, D. Tang, A. Ingram, H. Ly, K. Tai, L. Cai, J.W. Scholey, Flux through the hexosamine pathway is a determinant of nuclear factor kappaB-dependent promoter activation, Diabetes 51 (2002) 1146–1156.
[10] A. Golks, D. Guerini, The *O*-linked N-acetylglucosamine modification in cellular signaling and the immune system, EMBO reports 9 (2008) 748–753.
[11] Z.T. Kneasss, R.B. Marchase, Neutrophils exhibit rapid agonist-induced increases in protein-associated *O*-GlcNAc, J. Biol. Chem. 279 (2004) 45759–45765.
[12] A. Golks, T.T. Tran, J.E. Goetschy, D. Guerini, Requirement for *O*-linked *N*-acetylglucosaminyltransferase in lymphocytes activation, EMBO J. 26 (2007) 4368–4379.
[13] L.K. Kreppel, M.A. Blomberg, G.W. Hart, Dynamic glycosylation of nuclear and cytosolic proteins. Cloning and characterization of a unique *o*-GlcNAc transferase with multiple tetratricopeptide repeats, J. Biol. Chem. 272 (1997) 9308–9315.
[14] W.A. Lubas, D.W. Frank, M. Krause, J.A. Hanover, GlcNAc transferase is a conserved nucleocytoplasmic protein containing tertratricopeptide repeats, J. Biol. Chem. 272 (1997) 9316–9324.
[15] K.C. Sohn, S.-I. Do, Transcriptional regulation and *O*-GlcNAcylation activity of zebrafish OGT during embryogenesis, Biochem. Biophys. Res. Commun. 337 (2005) 256–263.
[16] L.M. Hartweck, C.L. Scott, N.E. Olszewski, Two *O*-linked *N*-acetylglucosamine transferase genes of Arabidopsis thaliana L. Heynh. Have overlapping functions necessary for gamete and seed development, Genetics 161 (2002) 1279–1291.
[17] D.A. Sinclair, M. Syrzycka, M.S. Macauley, T. Rastgardani, I. Komljenovic, D.J. Vocadlo, H.W. Brock, B.M. Honda, Drosophila-GlcNAc transferase (OGT) is encoded by the Polycomb group (PcG) gene, super sex combs (sxc), Proc. Natl. Acad. Sci. USA 106 (2009) 13427–13432.
[18] C. Janeway Jr., R. Medzhitov, Innate immunity, N. Eng. J. Med. 343 (2000) 338–344.
[19] S. Akira, K. Takeda, Toll-like receptor signaling, Nat. Rev. Immunol. 4 (2004) 499–511.
[20] L.J. Ignarro, Nitric Oxide Biology and pathology, Academic press, London, 2000.
[21] L.L. Daves, E. Martin, I.V. Turko, F. Murad, Novel effects of nitric oxide, Annu. Rev. Pharmacol. Toxicol 41 (2001) 203–236.
[22] J.S. Stamler, S. Lamas, F.C. Fang, Nitrosylation: the prototypic redox-based signaling mechanism, Cell 106 (2001) 675–683.
[23] A.J. Gow, Q. Chen, D.T. Hess, B.J. Day, H. Ischiropoulos, J.S. Stamler, Basal and stimulated protein *S*-nitrosylation in multiple cell types and tissues, J. Biol. Chem. 277 (2002) 9637–9640.
[24] Q.-W. Xie, Cloning and characterization of inducible nitric oxide synthase from mouse macrophages, Science 256 (1992) 225–228.
[25] S. Pfeiffer, A. Lass, K. Schmidt, B. Mayer, Protein tyrosine nitration in mouse peritoneal macrophages activated in vitro and in vivo evidence against an essential role of peroxynitrite, FASEB J. 15 (2001) 2355–2364.
[26] S.R. Jaffrey, H. Erdjument-Bromage, C.D. Ferris, P. Tempst, S.H. Snyder, Protein *S*-nitrosylation: a physiological signal for neuronal nitric oxide, Nat. Cell Biol. 3 (2001) 193–197.
[27] M.T. Forrester, M.W. Foster, J.S. Stamler, Assessment and application of the biotin switch technique for examining protein *S*-nitrosylation under conditions of pharmacologically induced oxidative stress, J. Biol. Chem. 282 (2007) 13977–13983.
[28] C.C. Wu, C. Thiemermann, Biological control and inhibition of induction of nitric oxide synthase, Methods Enzymol. 268 (1996) 408–420.
[29] J.B. Mannick, A. Hausladen, L. Limin, D.T. Hess, M. Zeng, Q.X. Miao, L.S. Kane, A.J. Gow, J.S. Stamler, Fas-induced caspase denitrosylation, Science 284 (1999) 651–654.
[30] Q. Li, I.M. Verma, NF_kB regulation in the immune system, Nat. Rev. Immunol. 2 (2002) 725–734.
[31] T.S. Lai, A. Hausladen, T.F. Slaughter, J.P. Eu, J.S. Stamler, C.S. Greenberg, Calcium regulates *S*-nitrosylation, denitrosylation and activity of tissue transglutaminase, Biochemistry 40 (2001) 4904–4910.
[32] G. Hao, B. Derakhshan, L. Shi, F. Campagne, S.S. Gross, SNOSID a proteomic method for identification of cysteine *S*-nitrosylation sites in complex protein mixtures, Proc. Natl. Acad. Sci. USA 103 (2006) 1012–1017.
[33] J.S. Paige, G. Xu, B. Stancevic, S.R. Jaffery, Nitrosothiol reactivity profiling identifies *S*-nitrosylated proteins with unexpected stability, Chem. Biol. 15 (2008) 1307–1316.
[34] L. Liu, A. Hausladen, M. Zeng, J. Heitman, J.S. Stamler, A metabolic enzyme for *S*-nitrosothiol conserved from bacteria to humans, Nature 410 (2001) 490–494.
[35] D.A. Mitchell, M.A. Marletta, Thioredoxin catalyzes the *S*-nitrosation of the caspase-3 active site cysteine, Nat. Chem. Biol. 1 (2005) 154–158.
[36] M. Benhar, M.T. Forrester, D.T. Hess, J.R. Stamler, Regulated protein denitrosylation by cytosolic and mitochondrial thioredoxins, Science 320 (2008) 1050–1054.